

H₂⁺ molecular ion in a strong magnetic field: Ground state

A. V. Turbiner* and J. C. López Vieyra†

Instituto de Ciencias Nucleares, UNAM, Apartado Postal 70-543, 04510 México, Distrito Federal, Mexico

(Received 16 November 2002; published 11 July 2003)

A detailed quantitative analysis of the system of two protons and one electron (ppe) placed in magnetic field ranging from 10^9 – 4.414×10^{13} G is presented. The present study is focused on the question of the existence of the molecular ion H₂⁺ in a magnetic field. A variational method with an optimization of the form of the vector potential (optimal gauge fixing) is used as a tool. It is shown that in the domain of applicability of the nonrelativistic approximation the (ppe) system in the Born-Oppenheimer approximation has a well-pronounced minimum in the total energy at a finite interproton distance for $B \leq 10^{11}$ G, thus manifesting the existence of H₂⁺. For $B \geq 10^{11}$ G and large inclinations (of the molecular axis with respect to the magnetic line) the minimum disappears and hence the molecular ion H₂⁺ does not exist. It is shown that the most stable configuration of H₂⁺ always corresponds to protons situated along the magnetic line. With magnetic field growth the H₂⁺ ion becomes more and more tightly bound and compact, and the electronic distribution evolves from a two-peak to a one-peak pattern. The domain of inclinations where the H₂⁺ ion exists reduces with magnetic field increase and finally becomes 0° – 25° at $B = 4.414 \times 10^{13}$ G. Phase-transition-type behavior of variational parameters for some interproton distances related to the beginning of the chemical reaction $H_2^+ \leftrightarrow H + p$ is found.

DOI: 10.1103/PhysRevA.68.012504

PACS number(s): 31.15.Pf, 31.10.+z, 32.60.+i, 97.10.Ld

I. INTRODUCTION

Many years have passed since the day when theoretical qualitative arguments were given that show that in the presence of a strong magnetic field the physics of atoms and molecules exhibits a wealth of new, unexpected phenomena even for the simplest systems [1,2]. In particular, the chance that unusual chemical compounds may be formed which do not exist without magnetic field, was mentioned. In practice, the atmosphere of neutron stars, which is characterized by the presence of enormous magnetic fields, 10^{12} – 10^{13} G, as well as other astronomical objects carrying large magnetic fields ($> 10^8$ G) provide a valuable paradigm where this physics could be realized. Recently the experimental data collected by the *Chandra* x-ray observatory revealed certain irregularities in the spectrum of an isolated neutron star 1E1207.4-5209. These irregularities can be interpreted as absorption features at ~ 0.7 keV and ~ 1.4 keV of possible atomic or molecular nature [3].

One of the first general features observed in standard atomic and molecular systems placed in a strong magnetic field is an increase of both total and binding energies, accompanied by a drastic shrinking of the electron localization length in both the longitudinal and the transverse directions. Naturally, this leads to a decrease of the equilibrium distance with magnetic field growth. This behavior can be considered to be a consequence of the fact that for large magnetic fields the electron cloud takes a needlelike form extended along the magnetic-field direction and the system becomes effectively

quasi-one-dimensional [2]. It is obvious that the phenomenon of quasi-one-dimensionality enhances the stability of standard atomic and molecular systems from the electrostatic point of view. In particular, molecules become elongated along the magnetic line, forming a type of linear molecular polymer (for details see Refs. [4,5]). It also hints at the occurrence of exotic atomic and molecular systems, which do not exist in the absence of a magnetic field. Motivated by these simple observations, it was shown in Refs. [6,7] that three and even four protons can be bound by one electron. This shows that exotic one-electron molecular systems H₃²⁺ and H₄³⁺ can exist in sufficiently strong magnetic fields in the form of linear polymers. However, the situation becomes much less clear (and also much less studied) when the nuclei are not aligned with the magnetic-field direction, and thus, in general, do not form a linear system. Obviously, such a study would be important for understanding the kinetics of a gas of molecules in the presence of a strong magnetic field. As a first step towards such a study, even the simplest molecules in different spatial configurations deserve attention. Recently a certain spatial configuration of H₃²⁺ was studied in detail [8]. It was shown that in the range of magnetic fields $10^8 < B < 10^{11}$ G the (pppe) system, with the protons forming an equilateral triangle perpendicular to the magnetic lines, has a well-pronounced minimum in the total energy for a certain size of triangle. The goal of the present work is to attempt an extensive quantitative investigation of the ground state of H₂⁺ in the framework of a single approach in its entire complexity: a wide range of magnetic-field strengths (0 – 4.414×10^{13} G), arbitrary (but fixed) orientation of the molecular axis with respect to the magnetic line, and arbitrary internuclear distances. We are going to carry out this study in the Born-Oppenheimer approximation at zero order—assuming protons to be infinitely heavy charged centers. In principle, when the molecular axis is perpendicular to the magnetic line, the (ppe) system acquires extra stability from the electrostatic point of view. Electrostatic repulsion of the classical

*On leave from the Institute for Theoretical and Experimental Physics, Moscow 117259, Russia. Electronic address: turbiner@nuclecu.unam.mx

†Electronic address: vieyra@nuclecu.unam.mx

protons is compensated for by the Lorentz force acting on them. The following paper [9] will be devoted to a study of the lowest excited states in the parallel configuration $1\sigma_u, 2\sigma_g, 1\pi_{g,u}$ ($m=1$) and $1\delta_{g,u}$ ($m=-2$).

It is well known that among the two stable one-electron systems that exist in the absence of a magnetic field—the H atom and H_2^+ —the molecular ion H_2^+ is more stable. It remains so in the presence of a constant magnetic field unless $B \gtrsim 10^{13}$ G, where the exotic ion H_3^{2+} appears to be the most bound (see Ref. [7]). The H_2^+ ion has been widely studied, both with and without the presence of a magnetic field, due to its importance in astrophysics, atomic and molecular physics, solid state and plasma physics (see Refs. [4–33], and references therein). The majority of the previous studies were focused on the case of the parallel configuration, where the angle between the molecular axis and the magnetic-field direction is zero, $\theta=0^\circ$. The only exception is Ref. [17], where a detailed quantitative analysis was performed for any θ but for a single magnetic field $B=1$ a.u. Previous studies were based on various numerical techniques, but the overwhelming majority used different versions of the variational method, including the Thomas-Fermi approach. As a rule, in these studies the nuclear motion was separated from the electronic motion using the Born-Oppenheimer approximation at zero order. At the quantitative level, the important feature of the H_2^+ ion that magnetic-field growth is always accompanied by an increase in the total and binding energies, as well as a shrinking of the equilibrium distance was observed. As a consequence, one is led to a striking conclusion about a sharp increase in the probability of nuclear fusion for H_2^+ in the presence of a strong magnetic field [10].

In the present study we will also use a variational method. Our considerations will be limited to a study of the 1_g state, which realizes the ground state of the system if the bound state exists [35]. We will construct state-of-the-art, non-straightforward, “adequate” trial functions consistent with a variationally optimized choice of vector potential. We should stress that a proper choice of the form of the vector potential is one of the crucial points that guarantee the adequacy and reliability of our considerations. In particular, a proper positioning of the gauge origin where the vector potential vanishes is drastically important, especially for large interproton distances. For the parallel configuration, $\theta=0^\circ$ the present work can be considered as an extension (and also a development) of our previous work [24]. It is necessary to emphasize that we encounter several unknown physical phenomena that occur when the molecular axis deviates from the magnetic-field direction. If the magnetic field is sufficiently strong, $B \gtrsim 10^{11}$ G, and the inclination θ is larger than a certain critical angle, the H_2^+ ion does not exist contrary to a prediction in Refs. [12,10,26]. This prediction was based on an improper gauge dependence of the trial functions which caused a significant loss of accuracy and finally led to a qualitatively incorrect result. We find that in the weak field regime the (ppe) system in the equilibrium position at any inclination, the electronic distribution peaks at the positions of the protons, while at large magnetic fields the electronic distribution

is characterized by single peak at the midpoint between two protons. This change from a two-peak to a one-peak configuration appears around $B \sim 10^{10}$ – 10^{11} G with a slight dependence on the inclination angle θ . From a physical point of view, the former means that the electron prefers to stay in the vicinity of a proton. This can be interpreted as dominance of the H-atom plus proton configuration. The latter situation implies that the electron is “shared” by both protons and hence such a separation into H-atom plus proton is irrelevant. Therefore, we can call the two-peak situation “ionic” coupling, while the one-peak case can be designated as “covalent” coupling, although this definition differs from that widely accepted in textbooks (see, for example, Ref. [34]). Thus, we can conclude that a phenomenon appears—as the magnetic field grows, the type of coupling changes from ionic to covalent. At large internuclear distances the electron is always attached to one of the charged centers, so the coupling is ionic.

One particular goal of our study is to investigate a process of dissociation of the (ppe) system: $H_2^+ \rightarrow H + p$ which appears with increase of interproton distance. It is clear from a physical point of view that at large distances the electronic distribution should be first of the two-peak type and then should change at asymptotically large distances to a single-peak one, but with a peak at the position of one of the protons. Somehow this process breaks permutation symmetry and we are not aware of any attempt to describe it. In our analysis this phenomenon appears as a consequence of a change of position of the gauge origin with increase of interproton distance.

From the physical point of view it is quite interesting to note how the (ppe) system behaves at very large interproton distances. This domain is modeled by an H-atom plus proton interaction. The interaction corresponds to (magnetic-field-inspired-quadrupole)+charge interaction and is dominant comparing to the standard Van der Waals force. For small inclinations the above interaction is attractive as in the Van der Waals case, but becomes *repulsive* for large inclinations. This implies that the potential curves approach the asymptotic value of the total energy at large interproton distances from above, in contradistinction to the Van der Waals case.

The Hamiltonian that describes two infinitely heavy protons and one electron placed in a uniform constant magnetic field directed along the z axis, $\mathbf{B}=(0,0,B)$, is given by (see, e.g., Ref. [34])

$$\mathcal{H} = \hat{p}^2 + \frac{2}{R} - \frac{2}{r_1} - \frac{2}{r_2} + (\hat{\mathbf{p}}\mathbf{A} + \mathbf{A}\hat{\mathbf{p}}) + \mathcal{A}^2 \quad (1)$$

(see Fig. 1 for notations), where $\hat{\mathbf{p}} = -i\nabla$ is the momentum, \mathbf{A} is a vector potential that corresponds to the magnetic field \mathbf{B} . Hence the total energy E_T of H_2^+ is defined as the total electronic energy plus the Coulomb energy of proton repulsion. The binding energy is defined as an affinity to having the electron at infinity, $E_b = B - E_T$. The dissociation energy is defined as an affinity to having a proton at infinity, $E_d = E_H - E_T$, where E_H is the total energy of the hydrogen atom in a magnetic field \mathbf{B} .

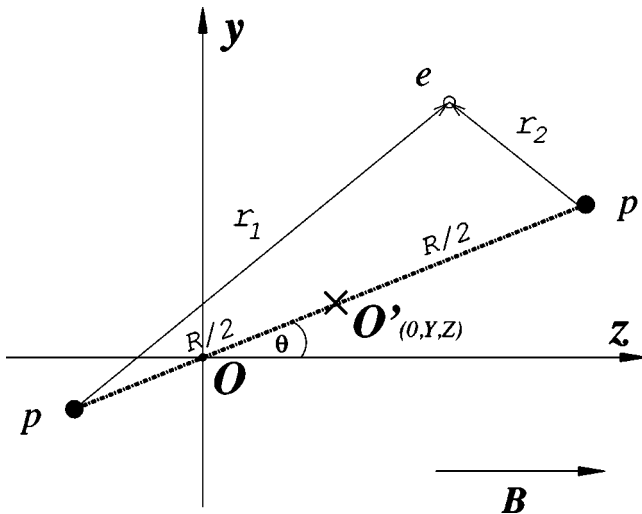


FIG. 1. Geometrical setting for the H₂⁺ ion placed in a magnetic field directed along the z axis. The protons are situated in the y-z plane at a distance R from each other and marked by bullets. O is the origin of coordinates, which is chosen to be on the bold-dashed line that connects the protons; O'(0,Y,Z) is the midpoint between the protons. It is assumed that the gauge center coincides with O. OO' measures the distance between the gauge center and the midpoint between the proton positions [see text and Eq. (4)].

Atomic units are used throughout ($\hbar = m_e = e = 1$), albeit energies are expressed in Rydbergs (Ry). Sometimes, the magnetic field B is given in a.u. with $B_0 = 2.35 \times 10^9$ G [36].

II. OPTIMIZATION OF THE VECTOR POTENTIAL

It is well known that the vector potential for a given magnetic field, even in the Coulomb gauge ($\nabla \cdot \mathbf{A} = 0$), is defined ambiguously, up to a gradient of an arbitrary function. This gives rise to a feature of gauge invariance: the Hermitian Hamiltonian is gauge covariant, while the eigenenergies and other observables are gauge independent. However, since we are going to use an approximate method for solving the Schrödinger equation with the Hamiltonian (1), our approximation of eigenenergies can well be gauge dependent (only the exact ones are gauge independent). Hence one can choose the form of the vector potential in a certain optimal way. In particular, if the variational method is used, the vector potential can be considered as a variational function and can be chosen by a procedure of minimization.

Let us consider a certain one-parameter family of vector potentials corresponding to a constant magnetic field $\mathbf{B} = (0,0,B)$

$$\mathbf{A} = B((\xi - 1)y, \xi x, 0), \quad (2)$$

where ξ is a parameter, in the Coulomb gauge. The position of the *gauge center* or *gauge origin*, where $\mathbf{A}(x,y,z) = 0$, is defined by $x = y = 0$, with z arbitrary. For simplicity we fix

$z = 0$. If $\xi = 1/2$, we get the well-known and widely used gauge which is called symmetric or circular. If $\xi = 0$ or 1, we get the asymmetric or Landau gauge (see Ref. [34]). By substituting Eq. (2) into Eq. (1), we arrive at a Hamiltonian of the form

$$\mathcal{H} = -\nabla^2 + \frac{2}{R} - \frac{2}{r_1} - \frac{2}{r_2} - 2iB[(\xi - 1)y\partial_x + \xi x\partial_y] + B^2[\xi^2 x^2 + (1 - \xi)^2 y^2], \quad (3)$$

where R is the interproton distance (see Fig. 1).

It is evident that for small interproton distances R the electron prefers to be near the midpoint between the two protons (coherent interaction with the protons). In the opposite limit, i.e., R large, the electron is situated near one of the protons (this is an incoherent situation—the electron selects and then interacts essentially with one proton). This fact, together with naive symmetry arguments, leads us to a natural assumption that the gauge center is situated on a line connecting the protons. Therefore the coordinates of the midpoint between the protons are

$$Y = \frac{Rd}{2} \sin \theta, \quad Z = \frac{Rd}{2} \cos \theta \quad (4)$$

(see Fig. 1), where d is a parameter. Thus, the position of the gauge center is effectively measured by the parameter d—a relative distance between the middle of the line connecting the protons and the gauge center. If the midpoint coincides with the gauge center, then $d = 0$. On the other hand, if the position of a proton coincides with the gauge center, then $d = 1$ or $d = -1$. Hence parameter d makes sense as a parameter characterizing a gauge.

The idea of choosing an optimal (convenient) gauge has been widely exploited in quantum-field-theory calculations. It has also been discussed in quantum mechanics and, in particular, in connection with the present problem. Perhaps, the first constructive (and remarkable) attempt to realize the idea of an optimal gauge was made in the 1980s by Larsen [12]. In his variational study of the ground state of the H₂⁺ molecular ion it was explicitly shown that for a given fixed trial function the gauge dependence of the energy can be quite significant. Furthermore, even an oversimplified optimization procedure improves the accuracy of the numerical results [37].

Our present aim is to study the ground state of Eq. (1) or, more concretely, Eq. (3). We propose a different way of optimizing the vector potential than those discussed by previous authors. It can be easily demonstrated that for a one-electron system there always exists a certain gauge for which the ground-state eigenfunction is a real function. Let us fix a vector potential in Eq. (1). Assume that we have solved the spectral problem exactly and have found the ground-state eigenfunction. In general, it is a certain *complex* function with a nontrivial, coordinate-dependent phase. Treating this phase as a gauge phase and then gauging it away finally

results in a new vector potential. This vector potential has the property we want—the ground-state eigenfunction of the Hamiltonian (1) is real. It is obvious that similar considerations are valid for any excited state. In general, for a given eigenstate there exists a certain gauge in which the eigenfunction is real. For different eigenstates these gauges can be different. It is obvious that a similar situation occurs for any one-electron system in a magnetic field.

Dealing with real trial functions has an immediate advantage: the expectation value of the terms proportional to \mathbf{A} in Eq. (1) [or $\sim B$ in Eq. (3)] vanishes when it is taken over any real, normalizable function. Thus without loss of generality, the term $\sim B$ in Eq. (3) can be omitted. Thus, we can use real trial functions with explicit dependence on the gauge parameters ξ and d . *These parameters are fixed by performing a variational optimization of the energy.* Therefore, as a result of the minimization, we find both a variational energy and a gauge for which the ground-state eigenfunction is real, as well as the corresponding Hamiltonian. One can easily show that for a system possessing axial (rotational) symmetry [38] the optimal gauge is the symmetric gauge $\xi=1/2$ with arbitrary d . This is precisely the gauge that has been overwhelmingly used (without any explanation) in the majority of the previous research on H_2^+ in the parallel configuration [1–33]. However, this is not the case if $\theta \neq 0^\circ$. For the symmetric gauge the exact eigenfunction now becomes complex, therefore complex trial functions must be used. But, following the recipe proposed above, we can avoid complex trial functions by adjusting the gauge in such a way that the eigenfunction remains real. This justifies the use of real trial functions. Our results (see Sec. IV) lead to the conclusion that for the ground state the optimal gauge parameter varies in the $\xi \in [0.5, 1]$ interval.

III. CHOOSING TRIAL FUNCTIONS

The choice of trial functions contains two important ingredients: (i) a search for the gauge leading to the real, exact ground-state eigenfunction and (ii) performance of a variational calculation based on *real* trial functions. The main assumption is that a gauge corresponding to a real, exact ground-state eigenfunction is of type (2) (or somehow is close to it) [39]. In other words, one can say that we are looking for a gauge of type (2) which admits the best possible approximation of the ground-state eigenfunction by real functions. Finally, in regard to our problem, the following recipe of variational study is used: As the first step, we construct an adequate variational real trial function Ψ_0 [27], for which the potential $V_0 = \Delta\Psi_0/\Psi_0$ reproduces the original potential near Coulomb singularities and at large distances, where ξ and d would appear as parameters. The trial function should support the symmetries of the original problem. We then perform a minimization of the energy functional by treating the free parameters of the trial function and ξ, d on the same footing. In particular, such an approach enables us to find the *optimal* form of the Hamiltonian as a function of ξ, d .

For arbitrary orientation of the magnetic field with respect to internuclear axis, parity under the permutations of the

charged centers is conserved. In general, we refer to the lowest gerade and ungerade states in our study as 1_g and 1_u . This is the only unified notation that makes sense for all orientations $0^\circ \leq \theta \leq 90^\circ$.

The above recipe (for the symmetric gauge where $\xi = 1/2, d=0$) was successfully applied in a study of the H_2^+ ion in a magnetic field for the parallel configuration $\theta=0^\circ$ [24] and also for general one-electron linear systems aligned along the magnetic field [7]. In particular, this led to the prediction of the existence of the exotic ions H_3^{2+} at $B \geq 10^{10}$ G, and in a linear configuration H_4^{3+} at $B \geq 10^{13}$ G [6,7]. Recently this recipe was used for the first time to make a detailed study of the spatial configuration H_3^{2+} [8]. It was demonstrated that inconsistency between the form of vector potential and a choice of trial functions can lead to nontrivial artifacts such as the existence of spurious bound states (see Ref. [28]).

One of the simplest trial functions for the 1_g state which meets the requirements of our criterion of adequacy is

$$\Psi_1 = e^{-\alpha_1(r_1+r_2)} e^{-B[\beta_{1x}\xi x^2 + \beta_{1y}(1-\xi)y^2]} \quad (5)$$

(cf. Refs. [24,26]), where α_1 , β_{1x} , and β_{1y} are variational parameters and ξ is parameter of the gauge (2). The first factor in function (5), being symmetric under interchange of the charge centers $r_1 \leftrightarrow r_2$, corresponds to the product of two $1s$ -Coulomb orbitals centered on each proton. This is nothing but the celebrated Heitler-London approximation for the ground state $1\sigma_g$. The second factor is the lowest Landau orbital corresponding to the vector potential of the form given in Eq. (2). Thus function (5) can be considered as a modification of the free field Heitler-London function. Following the experience gained in studies of H_2^+ without a magnetic field it is natural to assume that Eq. (5) is adequate to describe interproton distances near equilibrium. This assumption will be checked (and eventually confirmed) *a posteriori*, after making concrete calculations (see Sec. IV).

Function (5) is an exact eigenfunction in the potential

$$\begin{aligned} V_1 = \frac{\nabla^2 \Psi_1}{\Psi_1} = & 2\alpha_1^2 - 2B[\beta_{1x}\xi + \beta_{1y}(1-\xi)] \\ & + 4B^2[\beta_{1x}^2 \xi^2 x^2 + \beta_{1y}^2 (1-\xi)^2 y^2] + 2\alpha_1^2 (\hat{n}_1 \cdot \hat{n}_2) \\ & + 4\alpha_1 B \left[\frac{\beta_{1x}\xi x^2 + \beta_{1y}(1-\xi)y(y-y_1)}{r_1} \right. \\ & \left. + \frac{\beta_{1x}\xi x^2 + \beta_{1y}(1-\xi)y(y-y_2)}{r_2} \right] - 2\alpha_1 \left[\frac{1}{r_1} + \frac{1}{r_2} \right], \end{aligned}$$

where $y_{1,2}$ are the y coordinates of protons (see Fig. 1). The potential V_1 reproduces the functional behavior of the original potential (3) near Coulombic singularities and at large distances. These singularities are reproduced exactly when $\beta_{1x} = \beta_{1y} = 1/2$ and $\alpha_1 = 1$.

One can construct another trial function that meets the requirements of our criterion of adequacy as well,

$$\Psi_2 = (e^{-\alpha_2 r_1} + e^{-\alpha_2 r_2}) e^{-B[\beta_{2x}\xi x^2 + \beta_{2y}(1-\xi)y^2]} \quad (6)$$

(cf. Refs. [24,26]). This is the celebrated Hund-Mulliken function of the free field case multiplied by the lowest Landau orbital, where α_2 , β_{2x} , and β_{2y} are variational parameters. From a physical point of view this function has to describe the interaction between a hydrogen atom and a proton (charge center), and, in particular, models the possible dissociation mode of H₂⁺ into a hydrogen atom plus proton. Thus, one can naturally expect that for sufficiently large internuclear distances R this function prevails, giving a dominant contribution. Again this assumption will be checked *a posteriori*, by concrete calculations (see Sec. IV).

There are two natural ways to incorporate the behavior of the system in both regimes—near equilibrium and at large distances—into a single trial function. This is to make a linear or a nonlinear interpolation. The linear interpolation is given by a linear superposition

$$\Psi_{3a} = A_1 \Psi_1 + A_2 \Psi_2, \quad (7)$$

where A_1 or A_2 are parameters and one of them is kept fixed by the normalization condition. In turn the simplest nonlinear interpolation is of the form

$$\Psi_{3b} = (e^{-\alpha_3 r_1 - \alpha_4 r_2} + e^{-\alpha_3 r_2 - \alpha_4 r_1}) e^{-B[\beta_{3x}\xi x^2 + \beta_{3y}(1-\xi)y^2]} \quad (8)$$

(cf. Refs. [24,26]), where α_3 , α_4 , β_{3x} , and β_{3y} are variational parameters. This is a Guillemin-Zener function for the free field case multiplied by the lowest Landau orbital. If $\alpha_3 = \alpha_4$, function (8) coincides with Eq. (5). If $\alpha_4 = 0$, function (8) coincides with Eq. (6).

The most general ansatz is a linear superposition of the trial functions (7) and (8),

$$\Psi = A_1 \Psi_1 + A_2 \Psi_2 + A_3 \Psi_{3b}, \quad (9)$$

where we fix one of the A 's and let all the other parameters vary. Finally, the total number of variational parameters in Eq. (9), including R, ξ, d , is 15 for the ground state. For the parallel configuration, $\theta = 0^\circ$, the parameters $\xi = 0.5, d = 0$ are fixed in advance and also $\beta_{1x} = \beta_{1y}, \beta_{2x} = \beta_{2y}, \beta_{3x} = \beta_{3y}$. Hence the number of free parameters is reduced to ten for the ground state. Finally, with function (9) we intend to describe the ground state for *all* magnetic fields where nonrelativistic considerations are valid, $B \leq 4.414 \times 10^{13}$ G, and for *all* orientations of the molecular axis.

Calculations were performed using the minimization package MINUIT from CERN-LIB. Numerical integrations were carried out with a relative accuracy of $\sim 10^{-7}$ by use of the adaptive NAG-LIB (D01FCF) routine. All calculations were performed on a PC Pentium-III 800 MHz.

IV. RESULTS

We carry out a variational study of the (ppe) system with infinitely heavy protons in the range of magnetic fields $0 < B < 4.414 \times 10^{13}$ G, inclinations $0^\circ - 90^\circ$, for a wide range of interproton distances. For magnetic fields $B < 10^{11}$ G the

system displays a well-pronounced minimum in the total energy at *all* inclinations. However, for $B > 10^{11}$ G at large inclinations the minimum in the total energy disappears, while for small inclinations a minimum continues to exist. This picture describes the domain of existence of the molecular H₂⁺ ion. In general we confirm a qualitative result by Khersonskij [10] about the *nonexistence* of a minimum at finite distances on the total-energy surfaces of the (ppe) system at sufficiently strong magnetic fields for some far from parallel orientations. It is worth mentioning that the variational study in Ref. [10] was carried out with a trial function somewhat similar to that of Eq. (6), which, however, does not fully fulfill our criterion of adequacy. The potential corresponding to this function correctly reproduces the original potential near Coulomb singularities and $\sim \rho^2$ growth at large distances. However, it generates growing terms $\sim \rho$, which implies a reduction of the rate of convergence of a perturbation theory for which the variational energy represents the first two terms (see the discussion in Ref. [27]). Also, this trial function is not satisfactory from the point of view of gauge invariance. However, in spite of all the above-mentioned deficiencies it led to a qualitatively correct picture.

In Figs. 2–5 the total energy E_T of the (ppe) system as a function of interproton distance R for several values of the magnetic-field strength and different values of the inclination θ is shown. For magnetic fields $B \leq 10^{11}$ G and for all inclinations $0^\circ - 90^\circ$, each plot displays a well-pronounced minimum at $R = R_{eq}$, manifesting the existence of the molecular system H₂⁺. For $B = 1$ a.u. and $R \leq 3.5$ a.u. (see Fig. 2) our results are similar to the results of Refs. [15,17]—for fixed R the potential energy E_T grows with inclination. In general, at large $R > R_{eq}$ and for $\theta > 0^\circ$ all the curves behave alike: they have a maximum $R = R_{max}$ and then tend (from above) to the total energy of the hydrogen atom. The position of the maximum moves to larger distances with a decrease of the inclination. Eventually R_{max} tends to infinity at small inclinations. For $\theta = 0^\circ$ all potential curves approach to their asymptotic values from below, displaying, in general, a behavior similar to the field-free case, i.e., to Van der Waals-force-inspired behavior. This behavior is related to the fact that at large R the configuration H-atom+proton appears. The H atom has quadrupole moment, $Q \sim B^2$ (see Refs. [27,31–33]). Hence at large distances the total energy is dominated by a quadrupole-charge interaction and the long-range expansion has the form

$$E_T = -\frac{eQ(B)P_2(\cos \theta)}{R^3} - \frac{\alpha_H(B)}{2R^4} + \dots, \quad (10)$$

where P_2 is the second Legendre polynomial. In principle, the polarizability of the H atom by the proton, α_H , can depend on the magnetic field, but we are not aware of such a study. Using these two terms in Eq. (10) in order to describe the behavior of the potential curves in Figs. 2–5, one can extract information about $\alpha_H(B)$. At small inclinations $P_2(\cos \theta)$ is positive, the total energy is negative, thus corresponding to attraction between the quadrupole and the

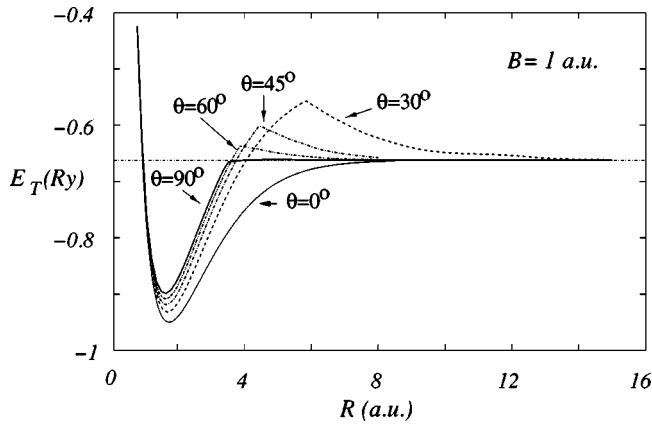


FIG. 2. Total energy E_T in rydbergs of the (ppe) system as a function of interproton distance R for different inclinations at $B = 2.3505 \times 10^9$ G (1 a.u.).

charge. Therefore, the total-energy curve approaches to the asymptotics from below. For large inclinations, $P_2(\cos \theta)$ is negative and the total energy is positive. Thus, this corresponds to repulsion between quadrupole and charge, and implies an existence of maximum of the total energy for large interproton distances $R > R_{eq}$. We observe the maximum in all Figs. 2–5. It is worth mentioning that in the calculations [15,17] for $B = 1$ a.u. and $\theta = 90^\circ$ (and other inclinations) the maximum was not observed in contradiction to our predictions (see Fig. 2 and also below Fig. 9). Looking at Fig. 2 it is interesting to compare a rate with which potential curves are approaching to the asymptotic total energy at large R . This asymptotic energy is equal to the total energy of the hydrogen atom, $E_H = -0.6623$ Ry, while $E_T^{\theta=0^\circ}(R=8 \text{ a.u.}) = -0.6647$ (from below), $E_T^{\theta=45^\circ}(R=8 \text{ a.u.}) = -0.6576$ (from above), $E_T^{\theta=90^\circ}(R=8 \text{ a.u.}) = -0.6620$ (from above). Thus, any deviation does not exceed 1%. There exists a different manner of viewing these results. It can be treated as a demonstration of the quality of our trial function (9) but for the calculation of the total energy of the atom.

However, the situation is drastically different for $B > 10^{11}$ G, see Figs. 4 and 5. There exists a certain critical

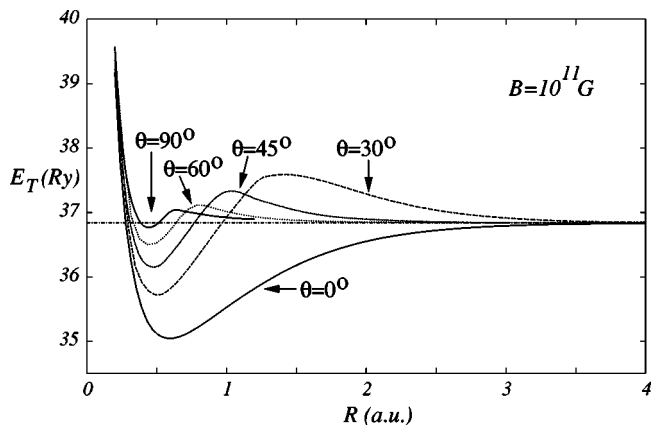


FIG. 3. Total energy E_T in rydbergs of the (ppe) system as a function of interproton distance R for different inclinations at $B = 10^{11}$ G.

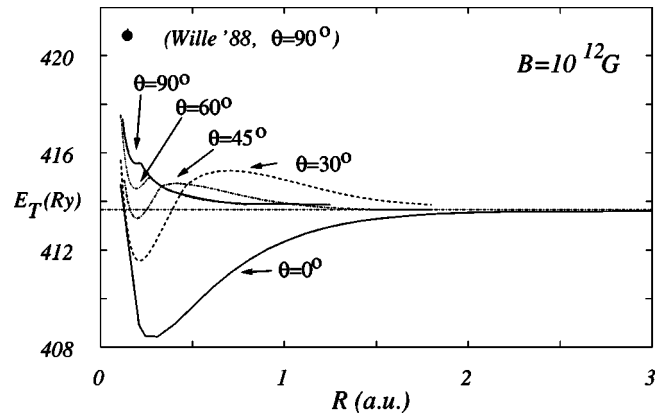


FIG. 4. Total energy E_T in rydbergs of the (ppe) system as a function of interproton distance R for different inclinations at $B = 10^{12}$ G. The result of Wille [15] is shown by a bullet (see text).

angle θ_{cr} , such that for $\theta < \theta_{cr}$ the situation remains similar to that given above—each potential curve is characterized by a well-pronounced minimum at finite R . With increase of the inclination, at $\theta \geq \theta_{cr}$ the minimum in the total energy first becomes very shallow with $E_T > E_H$ and ceases to exist at all. We were unable to localize with confidence the domain in R which corresponds to a shallow minimum which leads to the possible dissociation $H_2^+ \rightarrow H + p$ that was predicted in Ref. [12] as well as in our previous work [26]. We consider that the prediction of dissociation for large inclinations emerged as an artifact of an improper choice of the gauge fixing (see the discussion above). A detailed study of the transition domain (existence \leftrightarrow nonexistence) of H_2^+ is beyond the scope of the present paper. In any case, such a study requires much more accurate quantitative techniques as well as a sophisticated qualitative analysis. Schematically the situation is illustrated in Fig. 6.

It is quite interesting to explore the variation of the vector potential (2) for $\theta \neq 0^\circ$, in particular the position of the

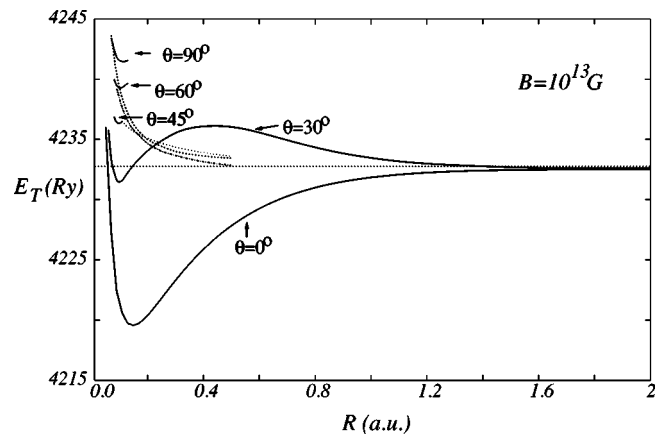


FIG. 5. Total energy E_T in rydbergs of the (ppe) system as a function of interproton distance R for different inclinations at $B = 10^{13}$ G. Plots for $\theta = 45^\circ, 60^\circ, 90^\circ$ consist of two parts: (i) (solid line), d kept fixed, $d = 0$ (gauge center coincides with the midpoint between the protons) which displays a minimum; and (ii) the dotted line is the result of minimization when the parameter d is released.

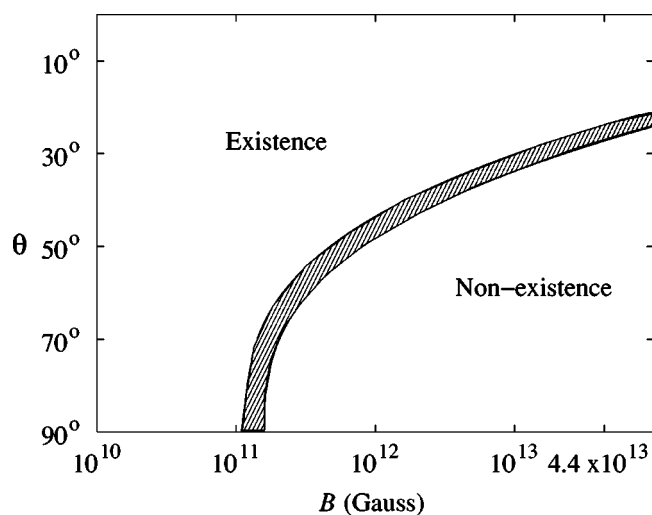


FIG. 6. H₂⁺ ion: domains of existence↔nonexistence for the 1_g state. The region filled by hatch marks illustrates the domain where the energy of the lowest rovibrational level is above the barrier and/or above the H+p asymptotic energy.

gauge center as a function of interproton distance R and magnetic field [40]. In Figs. 7(a) and 7(b) for $B=1$ a.u. and Figs. 8(a) and 8(b) for 10^{12} G, correspondingly, both the ξ and d dependences are presented [see Eq. (2) and discussion in Sec. III]. This dependence is very similar for all magnetic fields studied. It is worth emphasizing that for all the potential curves given, the minimum (in other words, the equilibrium position) at $R=R_{eq}$ somehow corresponds to a gauge close to the symmetric gauge: $\xi \approx 1/2$ [41] and $Y=Z=0$ ($d=0$). A similar situation holds for small interproton distances, $R < R_{eq}$. However, for large R , $R > R_{eq}$ the parameter ξ grows smoothly, reaching a maximum near the maximum of the potential curve which we denote by $R=R_{cr}$. It then falls sharply to the value $\xi \sim 1/2$. In turn, parameter d remains equal to 0 up to $R=R_{cr}$ (which means the gauge center coincides with the midpoint between protons), then sharply jumps to 1 (gauge center coincides with the position of a proton), displaying a behavior similar to a phase transition. It is indeed a type of *phase-transition* behavior stemming from symmetry breaking: from the domain $R < R_{cr}$, where the permutation symmetry of the protons holds and where the protons are indistinguishable, to the domain $R > R_{cr}$, where this symmetry does not exist and the electron is attached to one particular proton. Such a type of “phase transitions” is typical in chemistry and is called a “chemical reaction.” Hence the parameter R_{cr} characterizes a distance at which the chemical reaction $H_2^+ \rightarrow H+p$ starts. Somewhat similar behavior of the gauge parameters has appeared in the study of the exotic H_3^{2+} ion [8].

In Figs. 9 and 10 the behavior of the equilibrium distance R_{eq} , the position of the maximum R_{max} in the potential curves (see, for example, Figs. 2–5), and R_{cr} (see Figs. 7 and 8) vs inclination at $B=1$ a.u. and 10^{12} G are displayed. The calculations were performed for inclinations $0^\circ, 5^\circ, 15^\circ, 30^\circ, 45^\circ, 60^\circ, 75^\circ, 85^\circ$, and 90° . For both magnetic fields the behavior of R_{eq} vs θ demonstrates almost no dependence on θ in contrast to both R_{max} and R_{cr} which sharply decrease

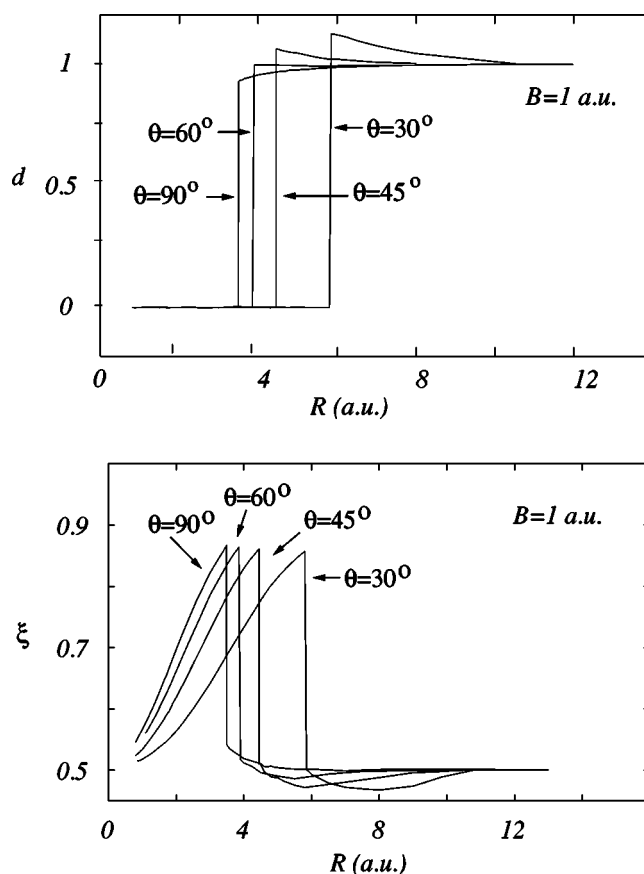


FIG. 7. (a) The dependence of d vs R at $B=1$ a.u. for different inclinations, $\theta \neq 0^\circ$. (b) The dependence of ξ vs R at $B=1$ a.u. for different inclinations, $\theta \neq 0^\circ$.

with the growth of θ . When inclination tends to zero R_{max} grows, corresponding eventually to the absence of a maximum at $\theta=0^\circ$. Similar behavior of R_{max} is observed for all studied magnetic fields. It is worth mentioning that at $B=1$ a.u. for almost all inclinations R_{cr} practically coincides with R_{max} . We do not have a reliable physical explanation of this behavior.

The total-energy dependence of H_2^+ (at $R=R_{eq}$) as a function of the inclination angle θ for different magnetic fields is shown in Fig. 11. The dotted line corresponds to the H-atom total energy in the corresponding magnetic field. For weak magnetic fields the hydrogen-atom total energy is always higher than that of the H_2^+ ion. However, for $B \geq 2 \times 10^{11}$ G the situation changes—a minimum of the H_2^+ total energy for angles $\theta > \theta_{cr}$ does not exist any more. Surprisingly, θ_{cr} corresponds approximately to the moment when the total energy of the H atom becomes equal to the total energy of the H_2^+ ion. If the form of the vector potential (2) is kept fixed with $\xi=1/2$ and $Y=Z=0$ ($d=0$), then a spurious minimum appears; its position is displayed by the dotted curve. However, if the gauge center parameters are released this minimum disappears (see the discussion above). This was the underlying reason for the erroneous statement about the existence of the unstable H_2^+ ion in this domain with a possible dissociation $H_2^+ \rightarrow H+p$ (see Ref. [26]). For all magnetic fields studied the total energy is minimal at θ

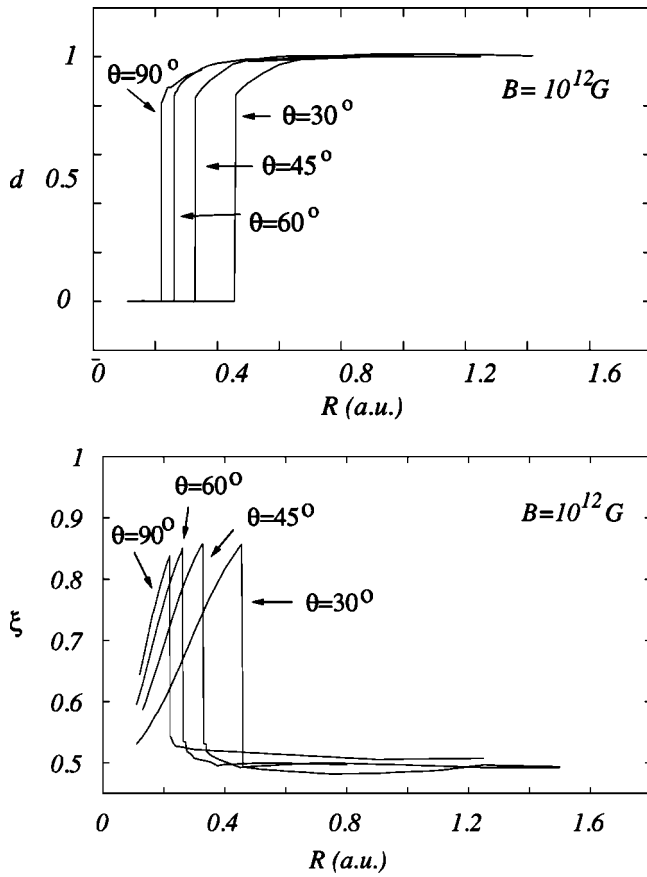


FIG. 8. (a) The dependence of d vs R at $B = 10^{12}$ G for different inclinations, $\theta \neq 0^\circ$. (b) The dependence of ξ vs R at $B = 10^{12}$ G for different inclinations, $\theta \neq 0^\circ$.

$= 0^\circ$ (parallel configuration) and then increases monotonically with inclination in complete agreement with the statements of other authors [10,12,15,17].

In a similar way the binding energy $E_b = B - E_T$, as well as the dissociation energy (affinity to a hydrogen atom) $E_d = E_H - E_T$ as a function of θ always decreases when changing from the parallel to the perpendicular configuration (see Fig. 11). Such behavior holds for all values of the magnetic-

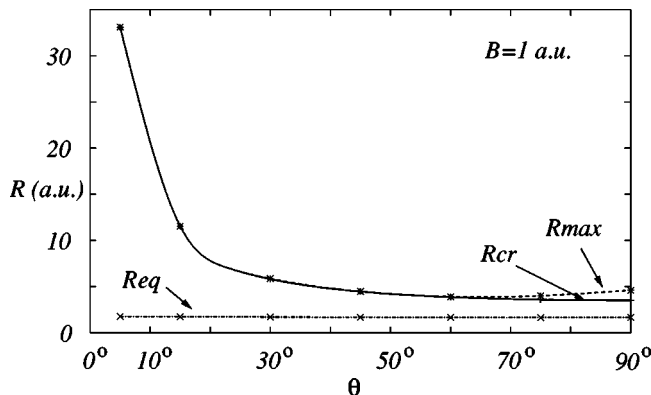


FIG. 9. The dependence of R_{crit} and the position of the maximum R_{max} compared to the equilibrium position R_{eq} at $B = 1$ a.u. for different inclinations θ .

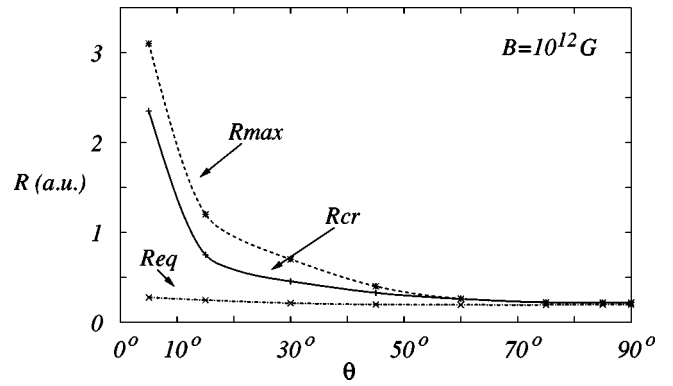


FIG. 10. The dependence of R_{crit} and the position of the maximum R_{max} compared to the equilibrium position R_{eq} at $B = 10^{12}$ G for different inclinations θ .

field strength studied. Thus we can draw the conclusion that the molecular ion becomes less and less stable monotonically as a function of the inclination angle. This confirms the statement made in Refs. [10,12,15,17] that the highest molecular stability of the 1_g state of H_2^+ occurs for the parallel configuration. Thus, the H_2^+ molecular ion is the most stable in parallel configuration.

We extend the validity of this statement to magnetic-field strengths $10^{13} < B \leq 4.414 \times 10^{13}$ G. It is worth emphasizing that the rate of increase of binding energy E_b with magnetic-field growth depends on the inclination—it slows down with increasing inclination. This effect implies that the H_2^+ ion in the parallel configuration becomes more and more stable against rotations—the energy of the lowest rotational state increases rapidly with magnetic field (see Table V below and the discussion there).

Regarding the interproton equilibrium distance R_{eq} , one would naively expect that it would always decrease with inclination (see Fig. 12). Indeed, for all the magnetic fields studied we observe that R_{eq} at $\theta = 0^\circ$ is larger than for any $\theta \neq 0^\circ$ (see below, Tables I–III). This can be explained as a natural consequence of the much more drastic shrinking of the electronic cloud in the direction transverse to the magnetic field than in the longitudinal direction. Actually, for magnetic fields $B \leq 10^{12}$ G the equilibrium distance R_{eq} decreases monotonically with inclination growth until it reaches θ_{cr} , as seen in Fig. 12. As mentioned above, if the parameters of the vector potential (2) are kept fixed, $\xi = 1/2$ and $Y = Z = 0$ ($d = 0$), a spurious minimum appears and generates anomalous (spurious) R_{eq} behavior for $\theta > \theta_{cr}$ (see Ref. [26]).

In Tables I, II, and III the numerical results for the total energy E_T , binding energy E_b , and equilibrium distance R_{eq} are displayed for $\theta = 0^\circ, 45^\circ$, and 90° , respectively. As seen in Table I, our results for $\theta = 0^\circ$ lead to the largest binding energies for $B > 10^{11}$ G in comparison with previous calculations. For $B \leq 10^{11}$ G, our binding energies for the parallel configuration appear to be very close (of the order of $\leq 10^{-4} - 10^{-5}$ in relative deviation) to the variational results of Wille [15], which are the most accurate so far in this region of magnetic-field strengths [42]. His results are based on the use of a trial function in the form of a linear superpo-

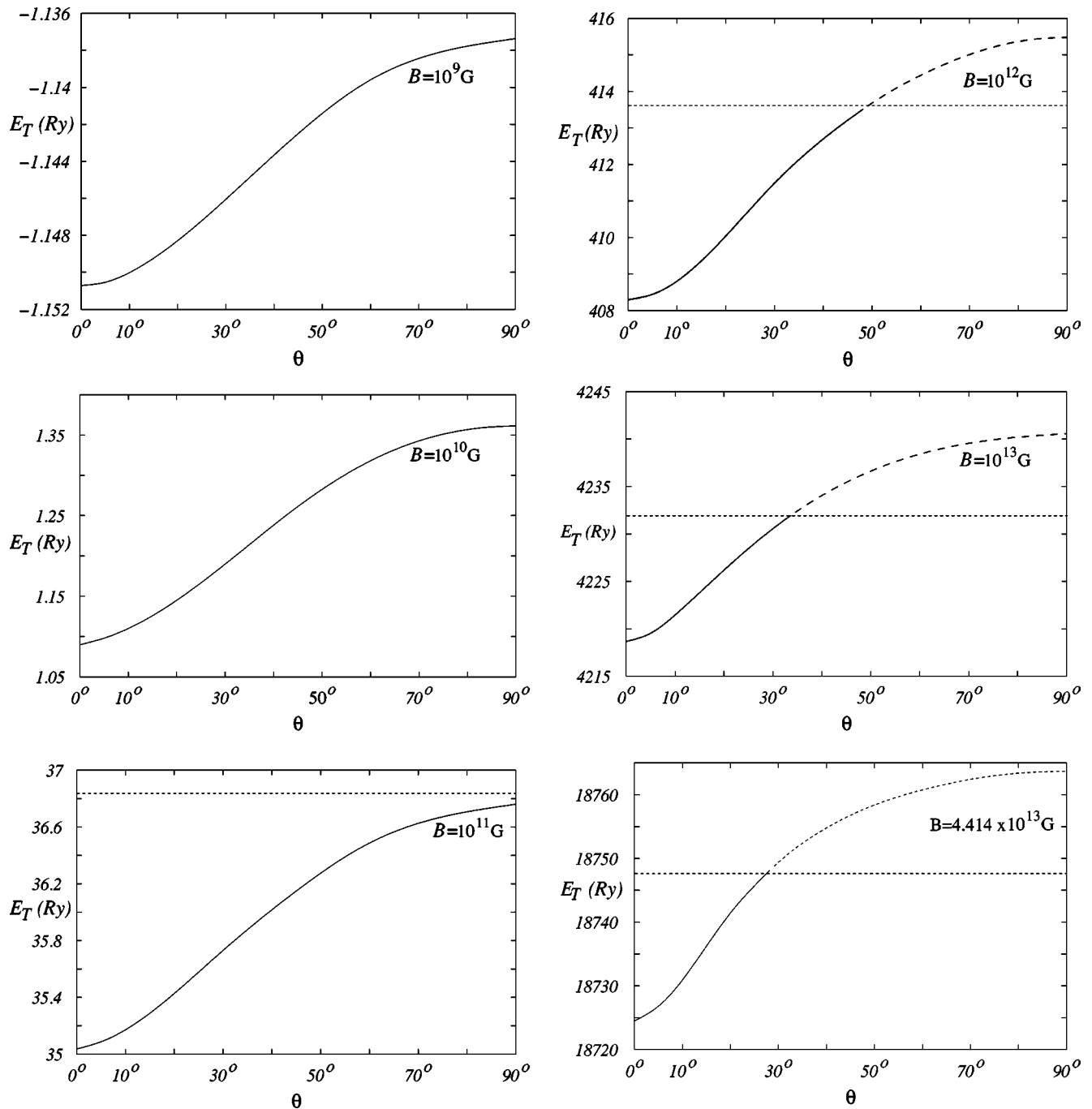


FIG. 11. H₂⁺ total energy E_T for the ground state 1_g at equilibrium $R=R_{eq}$ as a function of the inclination angle θ for different magnetic fields. The dotted lines correspond to the H-atom total energy taken from Ref. [22]. The dashed lines describe a total energy corresponding to a spurious minimum (see discussion in the text).

sition of ~ 500 Hylleraas-type functions. It is quite striking that our simple trial function (8) with ten variational parameters gives comparable (for $B \leq 10^{11}$ G) or even better (for $B > 10^{11}$ G) accuracy. It is important to discuss the reason why the trial function [15] fails to be increasingly inaccurate with magnetic-field growth for $B > 10^{11}$ G. An explanation of this inaccuracy is related to the fact that in the (x, y) directions the exact wave function decays asymptotically as a Gaussian function, unlike the Hylleraas functions that decay as the exponential of a linear function. The potential

corresponding to the function [15] reproduces correctly the original potential near Coulomb singularities but fails to reproduce $\sim \rho^2$ growth at large distances. This implies a zero radius of convergence of the perturbation theory for which the variational energy represents the first two terms (see the discussion in Ref. [27]).

The results for $\theta=45^\circ$ are shown in Table II, where a gradual shortening of the equilibrium distance is accompanied by an increase of total and binding energies with magnetic field. It is worth noting that parameter ξ evolves from

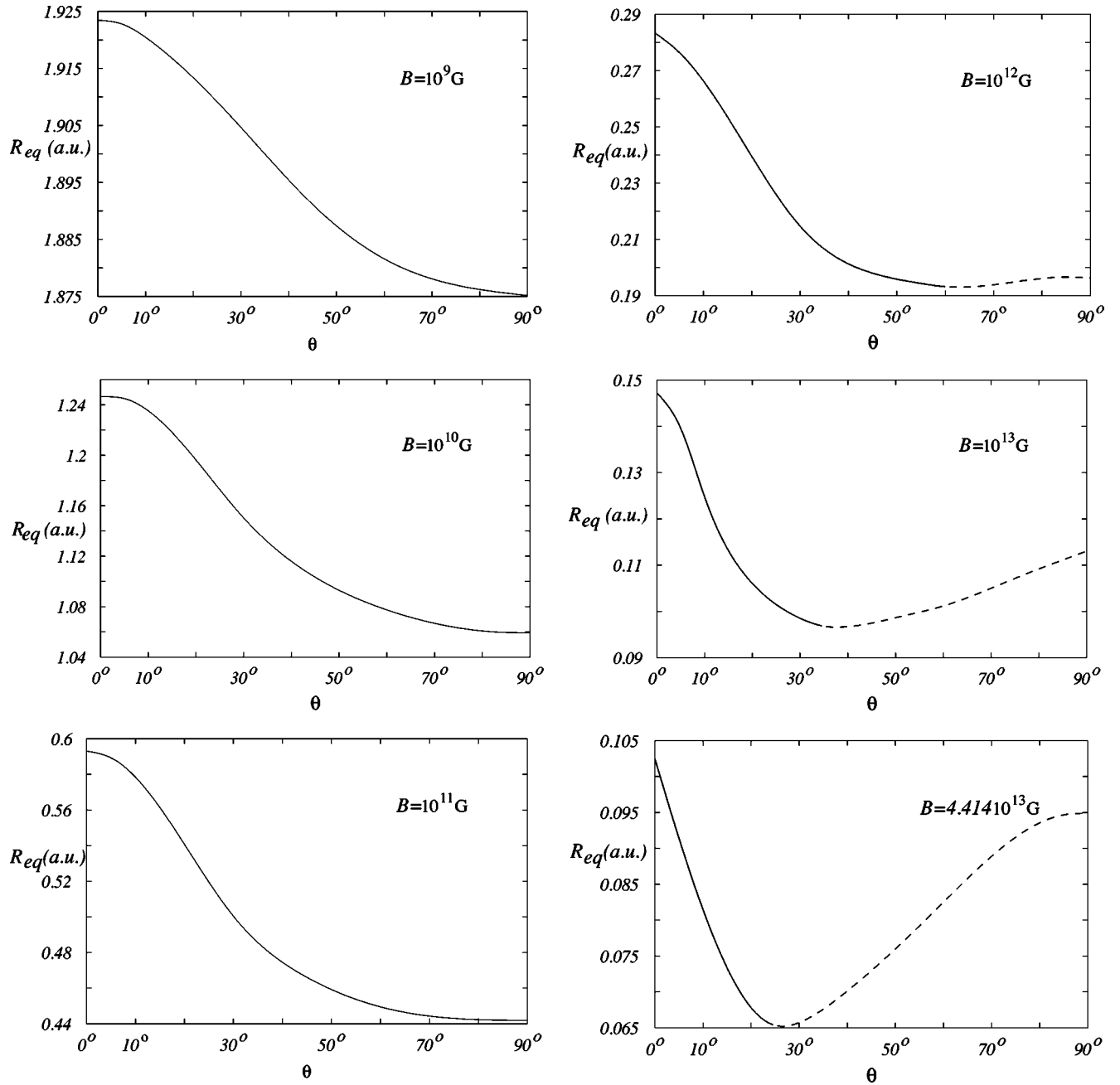


FIG. 12. H_2^+ equilibrium distance as a function of the inclination angle θ for the 1_g state. The dashed lines describe the position of a spurious minimum (see discussion in the text and Fig. 11).

about 0.5 to 0.93 with magnetic-field growth, thus changing from the symmetric gauge for weak fields to an almost asymmetric one for strong ones. This phenomenon occurs for all orientations $0 < \theta < \theta_{cr}$, becoming more and more pronounced with increasing inclination angle (see below). We are unaware of any other calculations for $\theta = 45^\circ$ to compare ours with.

For the perpendicular configuration $\theta = 90^\circ$, the results are presented in Table III. Similar to the parallel configuration case (see above), our results are again slightly less accurate than those of Wille [15] for $B \lesssim 10^{10}$ G, but become the most accurate results for stronger fields. In particular, this indicates that the domain of applicability of a trial function

in the form of a superposition of Hylleraas type functions becomes smaller as the inclination grows. The results reported by Larsen [12] and by Kappes and Schmelcher [17] are slightly worse than ours, although the difference is very small. The evolution of the gauge parameters follows a similar trend, as was observed at $\theta = 45^\circ$. In particular, ξ varies from 0.64 to 0.98 with magnetic-field growth from $B = 10^9$ G to $B \sim 2 \times 10^{11}$ G [43]. We should emphasize that the results of Larsen [12] and Wille [15] for $B > 10^{11}$ G do not seem relevant because of loss of accuracy, since the H_2^+ ion does not exist in this region.

In order to characterize the electronic distribution of H_2^+ for different orientations we have calculated the expectation

TABLE I. Total energy E_T , binding energy E_b , and equilibrium distance R_{eq} for the state 1_g in the parallel configuration, $\theta=0^\circ$.

B	E_T (Ry)	E_b (Ry)	R_{eq} (a.u.)		
$B=0$	-1.20525	1.20525	1.9971	Present ^a	
	-1.20527		1.997	Wille [15]	
10^9 G	-1.15070	1.57623	1.924	Present	
	-1.15072	1.57625	1.924	Wille [15]	
1 a.u.	-0.94991	1.94991	1.752	Present	
		1.9498	1.752	Larsen [12]	
		-0.94642	1.94642	1.76	Kappes and Schmelcher [17]
10^{10} G	1.09044	3.16488	1.246	Present	
		1.09031	3.16502	1.246	Wille [15]
10 a.u.	5.65024	4.34976	0.957	Present	
		4.35	0.950	Wille [15]	
		4.35	0.958	Larsen [12]	
		4.3346	0.950	Vincke and Baye [13]	
10^{11} G	35.0434	7.50975	0.593	Present	
		35.0428	7.5104	0.593	Wille [15]
			7.34559	0.61	Lai <i>et al.</i> [22]
100 a.u.	89.7090	10.2904	0.448	Present	
		10.2892	0.446	Wille [15]	
		10.1577	0.455	Wunner <i>et al.</i> [25]	
		10.270	0.448	Larsen [12]	
		10.2778	0.446	Vincke and Baye [13]	
10^{12} G	408.3894	17.1425	0.283	Present	
			17.0588	0.28	Lai <i>et al.</i> [22]
		408.566	16.966	0.278	Wille [15]
1000 a.u.	977.2219	22.7781	0.220	Present	
		21.6688	0.219	Wille [15]	
		22.7069	0.221	Wunner <i>et al.</i> [25]	
		22.67	0.222	Larsen [12]	
		22.7694	0.219	Vincke and Baye [13]	
10^{13} G	4219.565	35.7539	0.147	Present	
		4231.82	23.52	0.125	Wille [15]
			35.74	0.15	Lai <i>et al.</i> [22]
4.414×10^{13} G	18728.48	54.4992	0.101	Present	

^aThis value is taken from Ref. [24], where the variational method with the same trial function was used.

TABLE II. Total energy E_T , binding energy E_b , and equilibrium distance R_{eq} for the 1_g state at $\theta=45^\circ$. The optimal value of the gauge parameter ξ is given and $d=0$ is assumed (see text).

B	E_T (Ry)	E_b (Ry)	R_{eq} (a.u.)	ξ
10^9 G	-1.14248	1.56801	1.891	0.5806
1 a.u.	-0.918494	1.918494	1.667	0.5855
10^{10} G	1.26195	2.99337	1.103	0.5958
10 a.u.	6.02330	3.97670	0.812	0.6044
10^{11} G	36.15633	6.39686	0.466	0.6252
100 a.u.	91.70480	8.29520	0.337	0.6424
10^{12} G	413.2987	12.2332	0.198	0.6890
1000 a.u.	985.1956	14.8044	0.147	0.7151

values of the transverse $\langle \rho \rangle$ and longitudinal $\langle |z| \rangle$ sizes of the electronic cloud (see Table IV). Their ratio is always limited,

$$\frac{\langle \rho \rangle}{\langle |z| \rangle} < 1,$$

and quickly decreases with magnetic-field growth, especially for small inclination angles. This reflects the fact that the electronic cloud has a more and more pronounced needlelike form oriented along the magnetic line, as was predicted in the classical papers [1,2]. The behavior of $\langle \rho \rangle$ itself does not display any unusual properties, smoothly decreasing with magnetic field, quickly approaching the cyclotron radius for

TABLE III. Total energy E_T , binding energy E_b , and the equilibrium distance R_{eq} for the 1_g state in the perpendicular configuration, $\theta=90^\circ$. The optimal value of the gauge parameter ξ is presented and d is kept fixed, $d=0$ (see text). We emphasize that the calculations carried out in Refs. [15] and [12] for magnetic fields 10^{12} G and 1000 a.u., correspondingly, make no sense since the bound state of the (*ppe*) system does exist (see discussion in the text).

B	E_T (Ry)	E_b (Ry)	R_{eq} (a.u.)	ξ	
10^9 G	-1.137342	1.56287	1.875	0.6380	Present
		1.56384	1.879		Wille [15]
1 a.u.	-0.89911	1.89911	1.635	0.6455	Present
		1.8988	1.634		Larsen [12]
		1.8977	1.65		Kappes and Schmelcher [17]
10^{10} G	1.36207	2.89324	1.059	0.6621	Present
		2.8992	1.067		Wille [15]
10 a.u.	6.23170	3.76830	0.772	0.6752	Present
		3.7620	0.772		Larsen [12]
10^{11} G	36.7687	5.78445	0.442	0.7063	Present
		5.6818	0.428		Wille [15]
100 a.u.	92.7346	7.26543	0.320	0.7329	Present
		7.229	0.320		Larsen [12]
10^{12} G					Present
		4.558	0.148		Wille [15]
1000 a.u.					Present
		11.58	0.1578		Larsen [12]

small inclinations and large magnetic fields. In turn, $\langle |z| \rangle$ monotonically decreases with inclination growth.

As already mentioned, the results of our analysis of the parallel configuration of H_2^+ turned out to be optimal for all magnetic fields studied, being characterized by the smallest total energy. Therefore, it makes sense to study the lowest vibrational and also the lowest rotational state (see Table V). In order to do this we separate the nuclear motion along the molecular axis near equilibrium in the parallel configuration (vibrational motion) and deviation in θ of the molecular axis from $\theta=0^\circ$ (rotational motion). The vicinity of the mini-

TABLE IV. The 1_g state: expectation values of the transverse $\langle \rho \rangle$ and longitudinal $\langle |z| \rangle$ sizes of the electron distribution for the H_2^+ ion in a.u. at different orientations and magnetic-field strengths. At $\theta=0^\circ$ the expectation value $\langle \rho \rangle$ almost coincides with the cyclotron radius of the electron.

B	$\langle \rho \rangle$			$\langle z \rangle$		
	0°	45°	90°	0°	45°	90°
10^9 G	0.909	1.002	1.084	1.666	1.440	1.180
1 a.u.	0.801	0.866	0.929	1.534	1.313	1.090
10^{10} G	0.511	0.538	0.569	1.144	0.972	0.848
10 a.u.	0.359	0.375	0.396	0.918	0.787	0.708
10^{11} G	0.185	0.193	0.205	0.624	0.542	0.514
100 a.u.	0.123	0.129	0.139	0.499	0.443	0.431
10^{12} G	0.060	0.065		0.351	0.324	
1000 a.u.	0.039	0.043		0.289	0.275	
10^{13} G	0.019			0.215		
4.414×10^{13} G	0.009			0.164		

um of the potential surface $E(\theta, R)$ at $\theta=0^\circ, R=R_{eq}$ is approximated by a quadratic potential, and hence we arrive at a two-dimensional harmonic-oscillator problem in the (R, θ) plane. Corresponding curvatures near the minimum define the vibrational and rotational energies (for precise definitions and discussion see, for example, Ref. [12]). We did not carry out a detailed numerical analysis, making only rough estimates of the order of 20%. For example, at $B=10^{12}$ G we obtain $E_{vib}=0.276$ Ry in comparison with $E_{vib}=0.259$ Ry given in Ref. [7], where a detailed variational analysis of the potential electronic curves was performed. Our estimates for the energy E_{vib} of the lowest vibrational state are in reasonable agreement with previous studies. In particular, we confirm a general trend of a considerable increase of vibrational frequency with the growth of B indicated for the first time by Larsen [12]. The dependence of the energy on magnetic field is much more pronounced for the lowest rotational state—it grows much faster than the vibrational one with magnetic field increase. This implies that the H_2^+ ion in the parallel configuration becomes more stable for larger magnetic fields (see the discussion above). From a quantitative point of view, the results obtained by different authors are not in good agreement. It is worth mentioning that our results agree for large magnetic fields ≥ 10 a.u. with the results of Le Guillou and Zinn-Justin [16], obtained in the framework of the so-called “improved static approximation,” but deviate drastically at $B=1$ a.u., being quite close to the results of Larsen [12] and Wille [14]. As for the energy of the lowest rotational state, our results are in good agreement with those obtained by other authors (see Table V).

TABLE V. Energies of the lowest vibrational (E_{vib}) and rotational (E_{rot}) electronic states associated with the 1_g state at $\theta=0^\circ$. The indices in Le Guillou and Zinn-Justin [16] are assigned to the “improved adiabatic approximation” (a) and to the “improved static approximation” (b).

B	E_T (Ry)	E_{vib} (Ry)	E_{rot} (Ry)	
10^9 G	−1.15070	0.013	0.0053	Present
		0.011	0.0038	Wille [14]
1 a.u.	−0.94991	0.015	0.0110	Present
			0.0086	Wille [14]
		0.014	0.0091	Larsen [12]
		0.013		Le Guillou and Zinn-Justin (a) [16]
10^{10} G	1.09044	0.014	0.0238	Le Guillou and Zinn-Justin (b) [16]
		0.028	0.0408	Present
		0.026	0.0308	Wille [14]
		0.045	0.0790	Present
10 a.u.	5.65024	0.040	0.133	Larsen [12]
		0.039		Le Guillou and Zinn-Justin (a) [16]
		0.040	0.0844	Le Guillou and Zinn-Justin (b) [16]
		0.087	0.2151	Present
10^{11} G	35.0434	0.087	0.2151	Present
100 a.u.	89.7096	0.133	0.4128	Present
		0.141	0.365	Larsen [12]
		0.13		Wunner <i>et al.</i> [25]
		0.128		Le Guillou and Zinn-Justin (a) [16]
		0.132	0.410	Le Guillou and Zinn-Justin (b) [16]
10^{12} G	408.389	0.276	1.0926	Present
		0.198	1.0375	Khersonskij [11]
1000 a.u.	977.222	0.402	1.9273	Present
		0.38	1.77	Larsen [12]
		0.39		Wunner <i>et al.</i> [25]
		0.366		Le Guillou and Zinn-Justin (a) [16]
10^{13} G	4219.565	0.388	1.916	Le Guillou and Zinn-Justin (b) [16]
		0.717	4.875	Present
		0.592	6.890	Khersonskij [11]
4.414×10^{13} G	18728.48	1.249	12.065	Present

In Fig. 13 we show the electronic distributions $\int dy |\psi(x,y,z)|^2$ for magnetic fields $10^9, 10^{10}, 10^{11}, 10^{12}$ G and different orientations for H₂⁺ in the equilibrium configuration, $R=R_{eq}$. It was already found explicitly [24] that at $\theta=0^\circ$ with magnetic field increase there is a change from ionic (two-peak electronic distribution) to covalent coupling (one-peak distribution). We find that a similar phenomenon holds for all inclinations. If for $B=10^9$ G, all electronic distributions are characterized by two peaks for all inclinations, then for $B=10^{12}$ G all distributions have a single sharp peak. The “sharpness” of the peak grows with magnetic field. Figure 13 also demonstrates how the change of the type of coupling appears for different inclinations—for larger inclinations a transition (two peak) \leftrightarrow (one peak) appears for smaller magnetic fields. It seems natural that for the perpendicular configuration $\theta=90^\circ$, where the equilibrium distance is the smallest, this change appears for even smaller magnetic field.

In Figs. 14–18 we present the evolution of the electronic distributions as a function of interproton distance R , for inclinations $0^\circ, 45^\circ$ at $B=1$ a.u. and 10^{12} G together with the R dependence for the inclination 90° at $B=1$ a.u. The values

of the magnetic fields are chosen to illustrate in the most explicit way the situation. In all figures a similar picture is seen: namely, at not very large magnetic fields $B \leq 10^{11}$ G and for all inclinations, the electronic distribution at small $R < R_{cr}$ is permutationally symmetric and evolves with increase of R from a one-peak to a two-peak picture with more and more clearly pronounced separated peaks. Then for $R = R_{cr}$ this symmetry is broken and the electron randomly chooses one of protons and prefers to stay in its vicinity. For $R \gg R_{cr}$ the electronic distribution becomes totally asymmetric, the electron loses its memory of the second proton. This signals that the chemical reaction $\text{H}_2^+ \rightarrow \text{H} + p$ has happened. For larger magnetic fields $B \geq 10^{11}$ G for $R < R_{cr}$ the electronic distribution is always single-peaked, a transition from a one-peak to a two-peak picture occurs for $R > R_{cr}$, where the electronic distribution is already asymmetric.

To complete the study of the 1_g state, we show in Fig. 19 the behavior of the variational parameters of the trial function (9) as a function of the magnetic-field strength for the optimal (parallel) configuration, $\theta=0^\circ$. In general, the behavior of the parameters is rather smooth and very slowly changing, even though the magnetic field changes by several orders of magnitude. This is in sharp contrast with the results

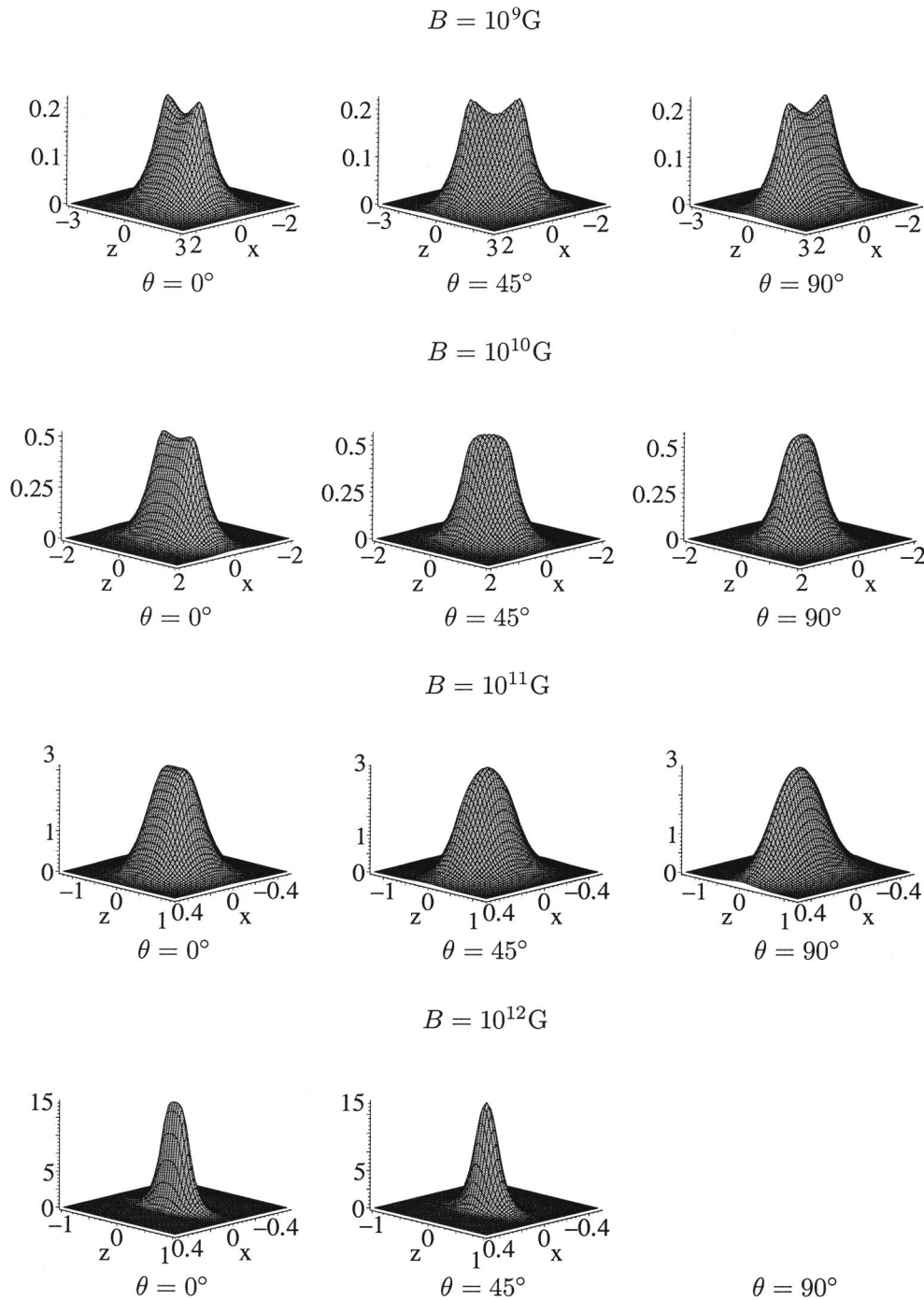


FIG. 13. Electronic distributions $\int dy |\psi(x,y,z)|^2$ (normalized to one) for the 1_g state of H_2^+ (equilibrium configuration) for different magnetic fields and inclinations.

of Kappes and Schmelcher [18] (see Fig. 1 in this paper). In our opinion such behavior of the parameters of our trial function (9) reflects the level of adequacy (or, in other words, indicates the quality) of the trial function. In practice, the parameters can be approximated by the spline method and then can be used to study magnetic-field strengths other than those presented here.

V. CONCLUSION

We have carried out an accurate, nonrelativistic calculation in the Born-Oppenheimer approximation for the lowest state of the H_2^+ molecular ion for different orientations of magnetic field with respect to the molecular axis. We studied constant uniform magnetic fields ranging from $B = 10^9$ G to

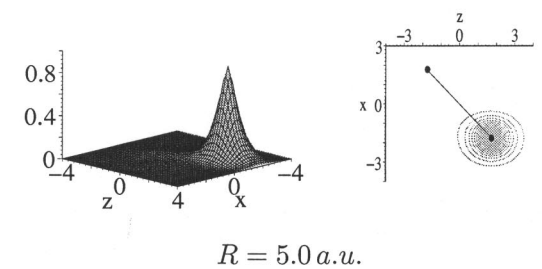
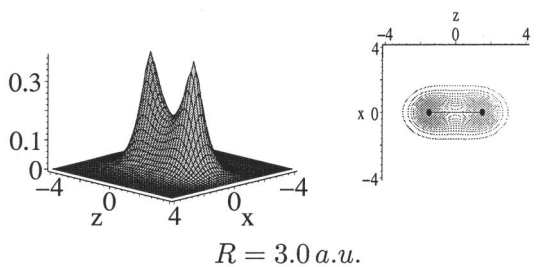
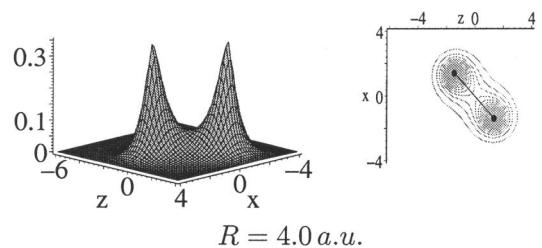
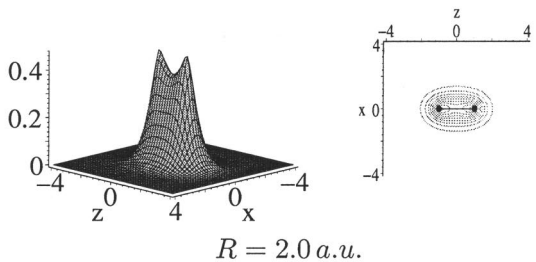
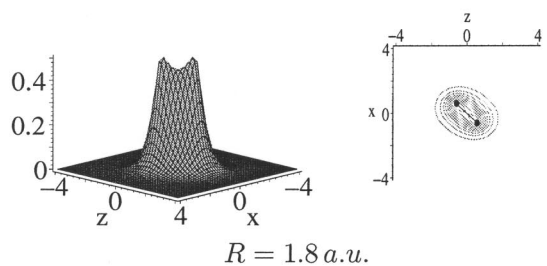
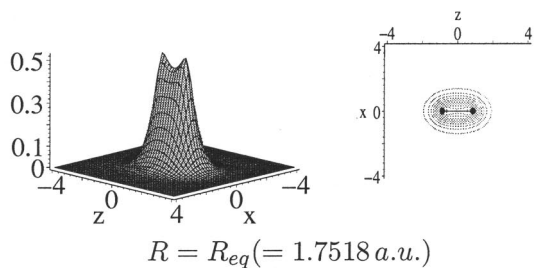
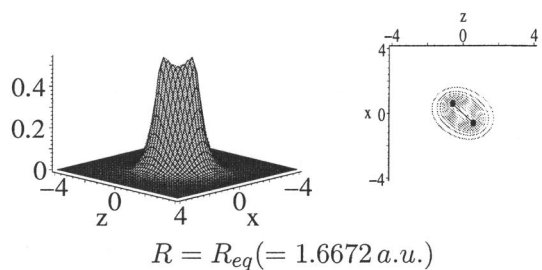
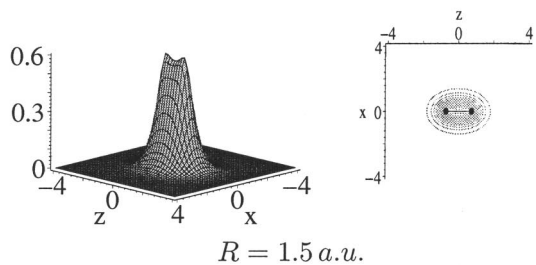
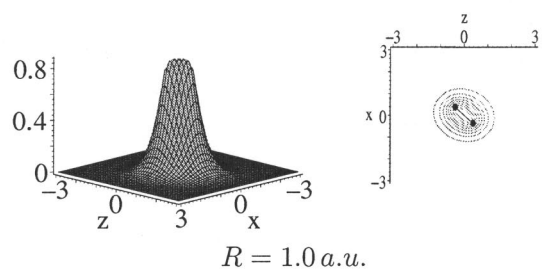
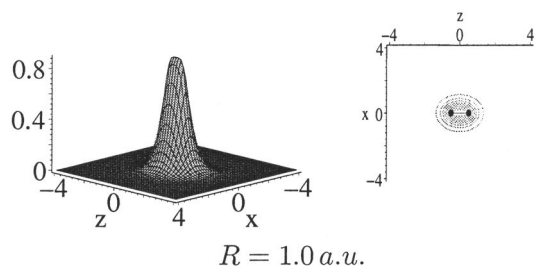


FIG. 14. Evolution of the electronic distributions $\int dy |\psi(x,y,z)|^2$ (normalized to one) and their contours for the 1_g state of the (ppe) system with interproton distance for $B=1$ a.u., $\theta=0^\circ$.

FIG. 15. Evolution of the electronic distributions $\int dy |\psi(x,y,z)|^2$ (normalized to one) and their contours for the 1_g state of the (ppe) system with interproton distance for $B=1$ a.u., $\theta=45^\circ$.

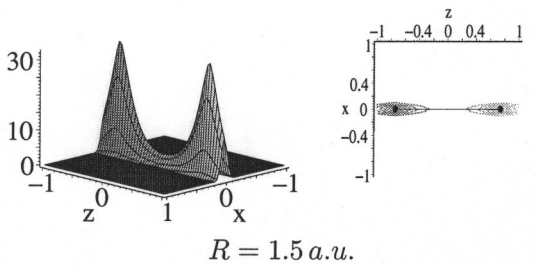
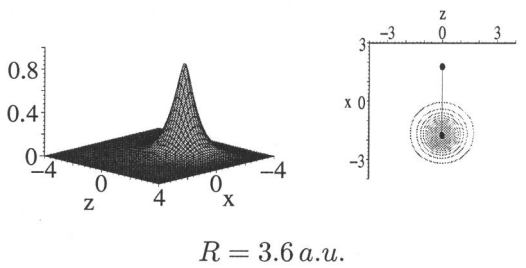
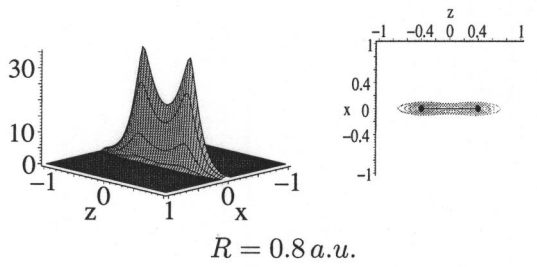
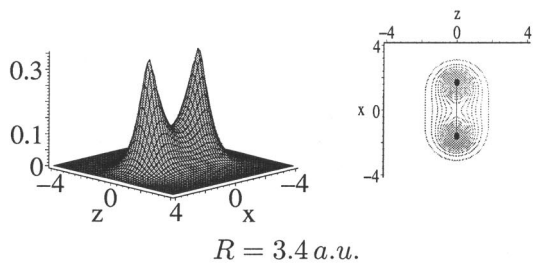
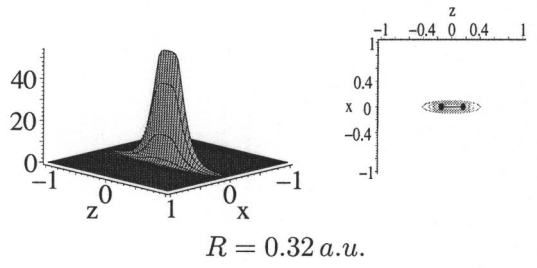
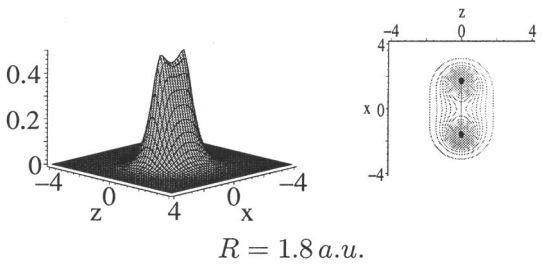
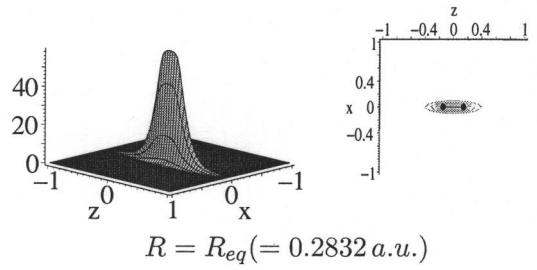
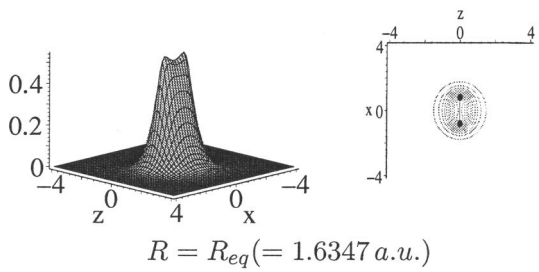
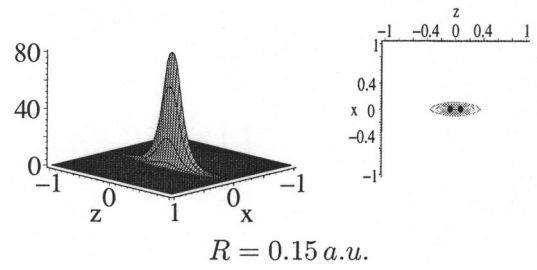
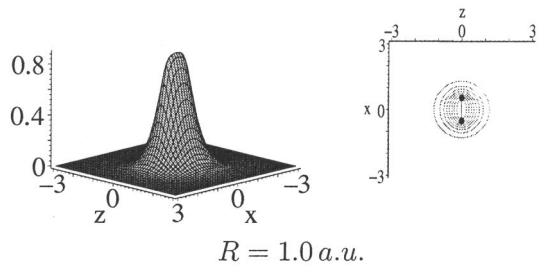


FIG. 16. Evolution of the electronic distributions $\int dy |\psi(x,y,z)|^2$ (normalized to one) and their contours for the 1_g state of the (ppe) system with interproton distance for $B=1 \text{ a.u.}$, $\theta=90^\circ$.

FIG. 17. Evolution of the electronic distributions $\int dy |\psi(x,y,z)|^2$ (normalized to one) and their contours for the 1_g state of the (ppe) system with interproton distance for $B=10^{12} \text{ G}$, $\theta=0^\circ$.

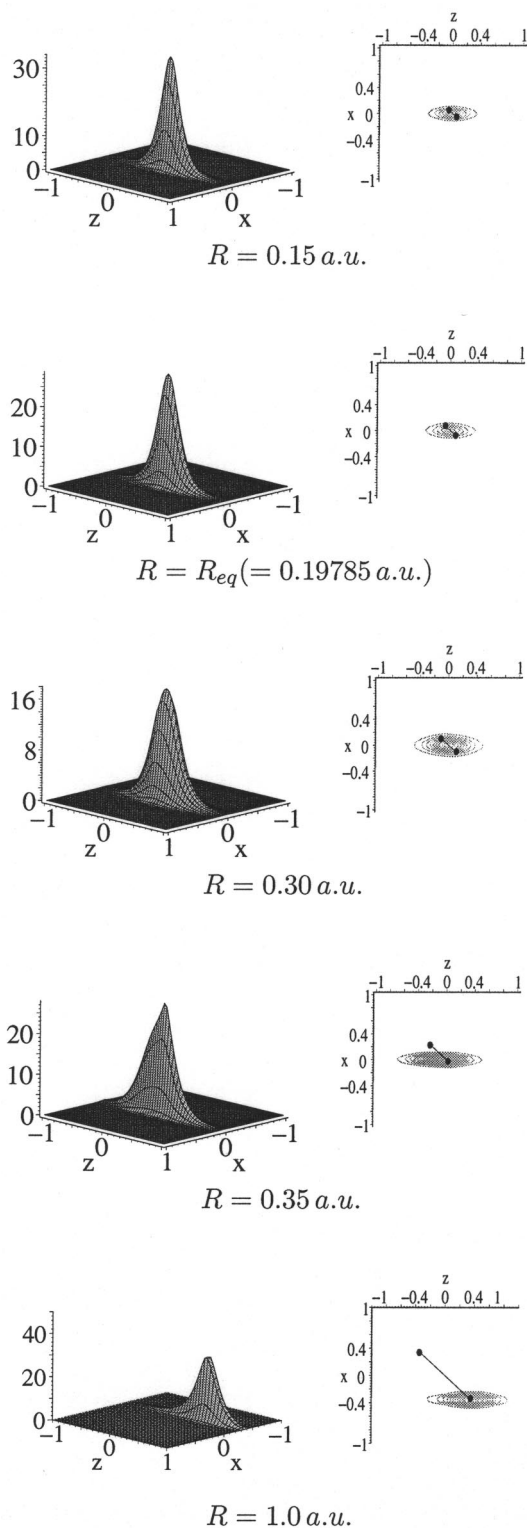


FIG. 18. Evolution of the electronic distributions $\int dy |\psi(x,y,z)|^2$ (normalized to one) and their contours for the 1_g state of the (ppe) system with interproton distance for $B=10^{12}$ G, $\theta=45^\circ$.

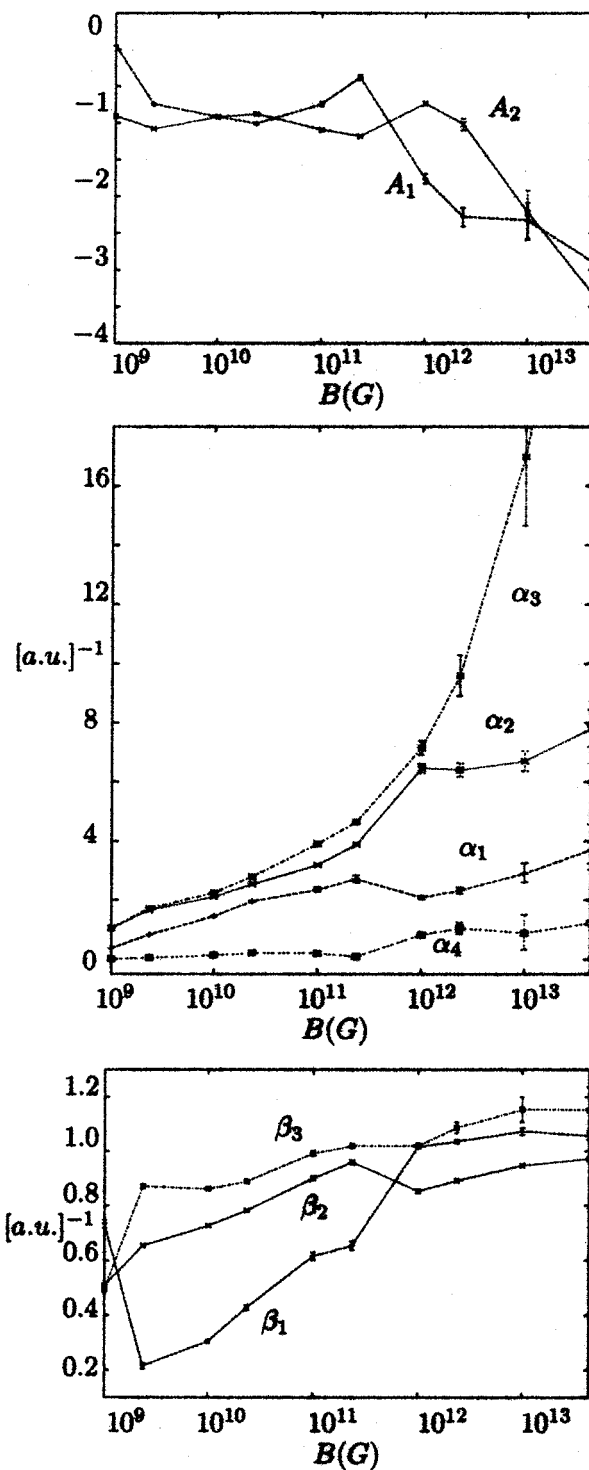


FIG. 19. Variational parameters of the trial function (9) as a function of the magnetic-field strength B for the 1_g state in the parallel configuration, $\theta=0^\circ$. In this case $\beta_1 = \beta_{1x}/2 = \beta_{1y}/2$, $\beta_2 = \beta_{2x}/2 = \beta_{2y}/2$, $\beta_3 = \beta_{3x}/2 = \beta_{3y}/2$ [see Eqs. (5), (6), and (8), cf. Ref. [24]]. The parameter A_3 is fixed to be 1, and $\xi = 1/2, d = 0$ (see text). The error bars correspond to the relative deviation in the variational energy in the region $\Delta E_T = E_T/E_{var} \leq 10^{-5}$.

$B = 4.414 \times 10^{13}$ G, where nonrelativistic considerations hold, although our method can be naturally applied to study the domain $B < 10^9$ G.

For all magnetic fields studied there exists a region of inclinations for which a well-pronounced minimum in the total energy surface for the 1_g state of the (ppe) system is found. This shows the existence of the H_2^+ molecular ion for magnetic fields $B = 0 - 4.414 \times 10^{13}$ G. The smallest total energy is always found to correspond to the parallel configuration, $\theta = 0^\circ$, where the protons are situated along the magnetic line. The total energy increases, while the binding energy decreases monotonically as the inclination angle grows. The rate of total-energy increase as well as binding-energy decrease is always seen to be maximal for the parallel configuration. The equilibrium distance exhibits quite natural behavior as a function of the orientation angle θ —for fixed magnetic field, shorter equilibrium distance always corresponds to larger θ .

Confirming the qualitative observations made by Khersonskij [10] for the 1_g state in contrast to statements in Refs. [12,15], we accurately demonstrate that the H_2^+ ion does not exist in a certain range of orientations for magnetic fields $B \geq 2 \times 10^{11}$ G. As the magnetic field increases, the region of inclinations where H_2^+ does not exist is seen to broaden, reaching a rather large domain $25^\circ \leq \theta \leq 90^\circ$ for $B = 4.414 \times 10^{13}$ G.

We find that the electronic distributions for H_2^+ in the equilibrium position are qualitatively different for weak and large magnetic fields. In the $B < 10^{10}$ G domain the electronic distribution for any inclination has a two-peak form, peaking near the position of each proton. On the contrary, for $B > 10^{11}$ G the electronic distribution always has a single-peak form with the peak near the midpoint between the pro-

tons for any inclination. This implies a physically different structure for the ground state—for weak fields the ground state can be modeled as a “superposition” of the hydrogen atom and proton, while for strong fields such modeling is not appropriate.

Unlike standard potential curves for molecular systems in the field-free case, we observe for $\theta > 0^\circ$ that each curve has a maximum and approaches the asymptotes at $R \rightarrow \infty$ from above. The electronic distribution evolves with R from a one-peak form at small R to a two-peak one at large R . There exists a certain critical R_{cr} at which one of the peaks starts to diminish, manifesting a breaking of permutation symmetry between the protons and simultaneously the beginning of the chemical reaction $H_2^+ \rightarrow H + p$.

Combining all the above-mentioned observations, we conclude that for magnetic fields of the order of magnitude $B \sim 10^{11}$ G some qualitative changes in the behavior of the H_2^+ ion take place. The behavior of the variational parameters also favors this conclusion. This hints at the appearance of a new scale in the problem.

ACKNOWLEDGMENTS

The authors wish to thank B. I. Ivlev and M. I. Eides for useful conversations and interest in the subject. We thank LPT, Universite Paris Sud, and ITAMP, Harvard University, where a part of the present work was done, for the kind hospitality extended to us. We thank M. Ryan for a careful reading of the manuscript. This work was supported in part by DGAPA Grant Nos. IN120199 and IN124202 and CONA-CyT Grant Nos. 36650-E and 25427-E (México). A.V.T. thanks the University Program FENOMECA (UNAM) and would like to acknowledge partial support from an NSF grant to ITAMP at Harvard University.

-
- [1] B.B. Kadomtsev and V.S. Kudryavtsev, Pis'ma Zh. Éksp. Teor. Fiz. **13**, 15 (1971) [JETP Lett. **13**, 9 (1971)]; Zh. Éksp. Teor. Fiz. **62**, 144 (1972) [Sov. Phys. JETP **35**, 76 (1972)].
- [2] M. Ruderman, Phys. Rev. Lett. **27**, 1306 (1971); *Physics of Dense Matter, Proceedings of the IAU Symposium*, edited by C. J. Hansen (Reidel, Dordrecht, 1974), Vol. 53, p. 117.
- [3] D. Sanwal *et al.*, Astrophys. J. Lett. **574**, L61 (2002).
- [4] R.H. Garstang, Rep. Prog. Phys. **40**, 105 (1977).
- [5] D. Lai, Rev. Mod. Phys. **73**, 629 (2001).
- [6] A. Turbiner, J.-C. López and U. Solis H., Pis'ma Zh. Éksp. Teor. Fiz. **69**, 800 (1999) [JETP Lett. **69**, 844 (1999)].
- [7] J.C. López Vieyra and A. Turbiner, Phys. Rev. A **62**, 022510 (2000).
- [8] J.C. López Vieyra and A. Turbiner, Phys. Rev. A **66**, 023409 (2002).
- [9] A. V. Turbiner and J. C. López Vieyra (unpublished).
- [10] V. Khersonskij, Astrophys. Space Sci. **98**, 255 (1984).
- [11] V. Khersonskij, Astrophys. Space Sci. **117**, 47 (1985).
- [12] D. Larsen, Phys. Rev. A **25**, 1295 (1982).
- [13] M. Vincke and D. Baye, J. Phys. B **18**, 167 (1985).
- [14] U. Wille, J. Phys. B **20**, L417 (1987).
- [15] U. Wille, Phys. Rev. A **38**, 3210 (1988).
- [16] J.C. Le Guillou and J. Zinn-Justin, Ann. Phys. (N.Y.) **154**, 440 (1984).
- [17] U. Kappes and P. Schmelcher, (a) Phys. Rev. A **51**, 4542 (1995); (b) **53**, 3869 (1996); (c) **54**, 1313 (1996); (d) Phys. Lett. A **210**, 409 (1996).
- [18] U. Kappes and P. Schmelcher, J. Chem. Phys. **100**, 2878 (1994).
- [19] D.R. Brigham and J.M. Wadehra, Astrophys. J. **317**, 865 (1987).
- [20] C.P. de Melo, R. Ferreira, H.S. Brandi, and L.C.M. Miranda, Phys. Rev. Lett. **37**, 676 (1976).
- [21] J.M. Peek and J. Katriel, Phys. Rev. A **21**, 413 (1980).
- [22] D. Lai, E. Salpeter, and S.L. Shapiro, Phys. Rev. A **45**, 4832 (1992).
- [23] D. Lai and E. Salpeter, Phys. Rev. A **53**, 152 (1996).
- [24] J.C. López Vieyra, P.O. Hess, and A. Turbiner, Phys. Rev. A **56**, 4496 (1997).
- [25] G. Wunner, H. Herold, and H. Ruder, Phys. Lett. **88A**, 344 (1982).
- [26] A.V. Turbiner, J.C. López Vieyra, and A. Flores R., Pisma Zh. Éksp. Teor. Fiz. **73**, 196 (2001) [JETP Lett. **73**, 176 (2001)].
- [27] A.V. Turbiner, Zh. Éksp. Teor. Fiz. **79**, 1719 (1980) [Sov. Phys.

- JETP **52**, 868 (1980)]; Usp. Fiz. Nauk. **144**, 35 (1984) [Sov. Phys. Uspekhi **27**, 668 (1984)]; Yad. Fiz. **46**, 204 (1987) [Sov. J. Nucl. Phys. **46**, 125 (1987)]; doctor of sciences thesis, ITEP, Moscow, 1989.
- [28] J.C. López Vieyra, Rev. Mex. Fis. **46**, 309 (2000).
- [29] Yu.P. Kravchenko, M.A. Liberman, and B. Johansson, Phys. Rev. A **54**, 287 (1996).
- [30] Yu.P. Kravchenko and M.A. Liberman, Phys. Rev. A **55**, 2701 (1997).
- [31] Yu.E. Lozovik and A.V. Klyuchnik, Phys. Lett. **66A**, 282 (1978).
- [32] A.V. Turbiner, Pisma Zh. Éksp. Teor. Fiz. **38**, 510 (1983) [JETP Lett. **38**, 618 (1983)].
- [33] A. Potekhin and A.V. Turbiner, Phys. Rev. A **63**, 065402 (2001).
- [34] L. D. Landau and E. M. Lifshitz, *Quantum Mechanics* (Pergamon, Oxford, 1977).
- [35] After a straightforward separation of the spin part of wave function, the original Schrödinger equation becomes a scalar Schrödinger equation. It can then be stated that a nodeless eigenfunction corresponds to the ground state (Perron theorem).
- [36] In the absence of convention, some results presented in literature are obtained for $B_0 = 2.3505 \times 10^9$ G. Thus, in making a comparison of the results obtained by different authors this fact should be taken into account.
- [37] For a review of different optimization procedures of the vector potential see, for instance, Ref. [18] and references therein.
- [38] This is the case whenever the magnetic field is directed along the molecular axis (parallel configuration).
- [39] This can be formulated as a problem—for a fixed value of B and a given inclination, find a gauge for which the ground-state eigenfunction is real.
- [40] At $\theta = 0^\circ$ (parallel configuration) the vector potential (2) remains unchanged, since $\xi = 1/2$.
- [41] The value of ξ grows with B [see Figs. 7(a) and 7(b) and below Tables II and III].
- [42] It is worth mentioning that for $B = 1$ a.u. and $R = 2$ a.u. our results are in good agreement with the accurate study performed in Ref. [30].
- [43] $\xi = 0.5$ at $B = 0$.